

# Anharmonic effects in thermoelectric and 2D materials

Unai Aseguinolaza Aguirreche

Supervised by Aitor Bergara and Ion Errea

August 31, 2020

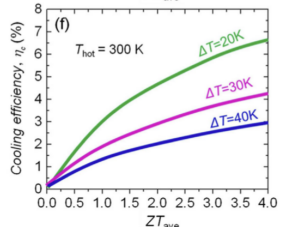
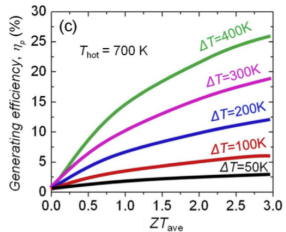
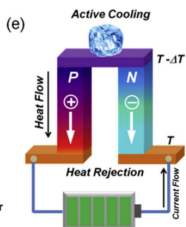
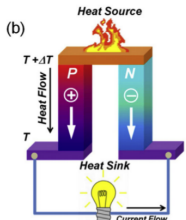


# Outline

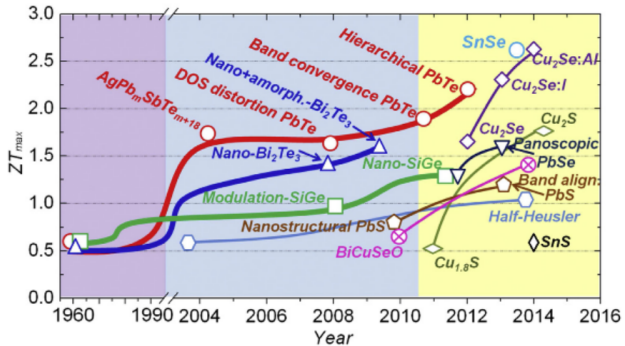
- Introduction
- Theoretical framework
- Part 1: Thermoelectric monochalcogenides
- Part 2: 2D materials
- Conclusions

# Introduction

$$ZT = \frac{S^2 \sigma T}{\kappa}, \quad S = -\frac{\Delta V}{\Delta T}$$



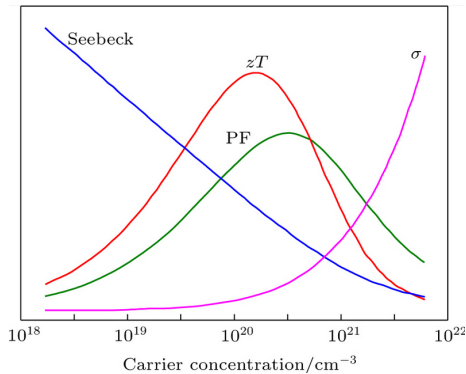
# Introduction



- $ZT_{max}$  low and in narrow temperature ranges
- Very limited technological applications.

X. Zhang, L-D. Zhao / Journal of Materomics 1 (2015) 92-105

# Introduction



- The physical magnitudes that define  $ZT$  are correlated
- How to overcome:
  - Doping + nanostructuring
  - Proximity to phase transitions
  - ...

### Ultralow thermal conductivity and high thermoelectric figure of merit in SnSe crystals

Li-Dong Zhao<sup>1</sup>, Shih-Han Lo<sup>2</sup>, Yongsheng Zhang<sup>2</sup>, Hui Sun<sup>3</sup>, Gangjian Tan<sup>1</sup>, Ctarad Uher<sup>3</sup>, C. Wolverton<sup>2</sup>, Vinayak P. Dravid<sup>2</sup> & Mercouri G. Kanatzidis<sup>1</sup>

The thermoelectric effect enables direct and reversible conversion between thermal and electrical energy, and provides a viable route for power generation from waste heat. The efficiency of thermoelectric materials is dictated by the dimensionless figure of merit,  $ZT$  (where  $Z$  is the figure of merit and  $T$  is absolute temperature), which governs the Carnot efficiency for heat conversion. Enhancements above the generally high threshold value of 2.5 have important implications for commercial deployment<sup>1–3</sup>, especially for compounds free of Pb and Te. Here we report an unprecedented  $ZT$  of  $2.6 \pm 0.3$  at 923 K, realized in SnSe single crystals measured along the  $b$  axis of the room-temperature orthorhombic unit cell. This material also shows a high  $ZT$  of  $2.3 \pm 0.3$  along the  $c$  axis but a significantly reduced  $ZT$  of  $0.8 \pm 0.2$  along the  $a$  axis. We attribute the remarkably high  $ZT$  along the  $b$  axis to the intrinsically ultralow lattice thermal conductivity in SnSe. The layered structure of SnSe derives from a distorted rock-salt structure, and features anomalously high Grüneisen parameters, which reflect the anharmonic and anisotropic bonding. We attribute the exceptionally low lattice thermal conductivity ( $0.23 \pm 0.03 \text{ W m}^{-1} \text{ K}^{-1}$  at 973 K) in SnSe to the anharmonicity. These findings highlight alternative strategies to nanostructuring for achieving high thermoelectric performance.

power factor (along the  $b$  axis), but, even more surprisingly, we observe that the thermal conductivity of SnSe is intrinsically ultralow ( $< 0.25 \text{ W m}^{-1} \text{ K}^{-1}$  at  $> 800 \text{ K}$ ), resulting in  $ZT = 2.62$  at 923 K along the  $b$  axis and 2.3 along the  $c$  axis; these represent the highest  $ZT$  values reported so far for any thermoelectric system. Along the  $a$  direction, however,  $ZT$  is significantly lower,  $\sim 0.8$ . Here, it should be noted that SnSe along the  $b$  axis shows a room-temperature  $ZT = 0.12$ , which is comparable to the room-temperature value of 0.15 reported earlier<sup>19</sup>. SnSe, however, reveals high  $ZT$  values near and above the transition temperature of 750 K at which the structure converts from  $Pnma$  to  $Cmcm$ <sup>20–22</sup>. Such ultrahigh  $ZT$  along two principal directions and the observed crystallographic and  $ZT$  anisotropy prompted us to investigate the scientific underpinning of these intriguing results.

SnSe adopts a layered orthorhombic crystal structure at room temperature, which can be derived from a three-dimensional distortion of the NaCl structure. The perspective views of the room-temperature SnSe crystal structure along the  $a$ ,  $b$  and  $c$  axial directions are shown in Fig. 1a–d. There are two-atom-thick SnSe slabs (along the  $b$ – $c$  plane) with strong Sn–Se bonding within the plane of the slabs, which are then linked with weaker Sn–Se bonding along the  $a$  direction<sup>20</sup>. The structure contains highly distorted  $\text{SnSe}_2$  coordination polyhedra, which have

- The best thermoelectric material so far: Intrinsic semiconductor with low lattice thermal conductivity ( $\kappa = \kappa_{el} + \kappa_l$ )

# Introduction

1 H									2 He								
3 Li	4 Be																
11 Na	12 Mg																
19 K	20 Ca	21 Sc	22 Ti	23 V	24 Cr	25 Mn	26 Fe	27 Co	28 Ni	29 Cu	30 Zn	31 Ga	32 Ge	33 As	34 Se	35 Br	36 Kr
37 Rb	38 Sr	39 Y	40 Zr	41 Nb	42 Mo	43 Tc	44 Ru	45 Rh	46 Pd	47 Ag	48 Cd	49 In	50 Sn	51 Sb	52 Te	53 I	54 Xe
55 Cs	56 Ba	*	72 Hf	73 Ta	74 W	75 Re	76 Os	77 Ir	78 Pt	79 Au	80 Hg	81 Tl	82 Pb	83 Bi	84 Po	85 At	86 Rn
87 Fr	88 Ra	+	104 Rf	105 Db	106 Sg	107 Bh	108 Hs	109 Mt	110 Ds	111 Rg	112 Uub	113 Uut	114 Uuq	115 Uup	116 Uuh	117 Uus	118 Uuo

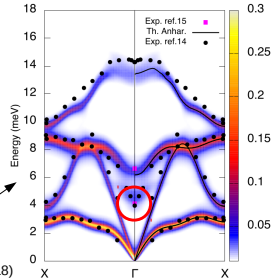
## Chalcogenides

Monochalcogenides: PbTe, SnTe, GeTe, SnS...

Low lattice thermal conductivity

They show strongly anharmonic features:

- Lattice instabilities in the harmonic phonons
- Ferroelectric transitions
- Incipient ferroelectricity
- Special features in the phonon spectral function



G. A. Ribeiro et al. Physical Review B 97, 014306 (2018)

# Theoretical framework

- Ionic Hamiltonian

$$H = T + V(\mathbf{R})$$

where  $\mathbf{R} = \mathbf{R}_0 + \mathbf{u}$ .

- Assuming that  $V(\mathbf{R})$  is well reproduced by a quadratic potential in the range of  $\mathbf{u}$ , Taylor expand the potential

$$V(\mathbf{R}) \simeq V(\mathbf{R}_0) + \frac{1}{2} \sum_{ab} \phi_{ab} u_a u_b + O(u^3)$$

where  $\phi_{ab} = \partial^2 V / \partial u_a \partial u_b|_0$ .

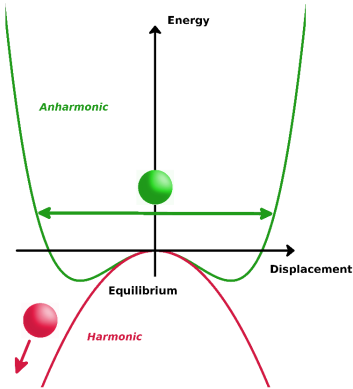
$$V^{harm}(\mathbf{R}) = V(\mathbf{R}_0) + \frac{1}{2} \sum_{ab} \phi_{ab} u_a u_b$$

- This Hamiltonian (Harmonic Hamiltonian) can be solved exactly.
- It provides well defined phonon quasiparticles

$$\sum_b \phi_{ab} \epsilon_\mu^b = M \omega_\mu^2 \epsilon_\mu^a$$

# Theoretical framework

- Harmonic approximation:
  - It does not work in monochalcogenides because they show harmonic instabilities.
- Perturbative approaches are not an option.
  - They are built on top of the harmonic theory.
- We apply a variational non-perturbative approach with anharmonic terms to infinite order: Stochastic self-consistent harmonic approximation (SSCHA)



## Theoretical framework

- SCHA is a method for approximating the vibrational free energy of a crystal.

$$F_H = \text{tr}(\rho_H H) + \frac{1}{k_B T} \text{tr}(\rho_H \ln \rho_H)$$

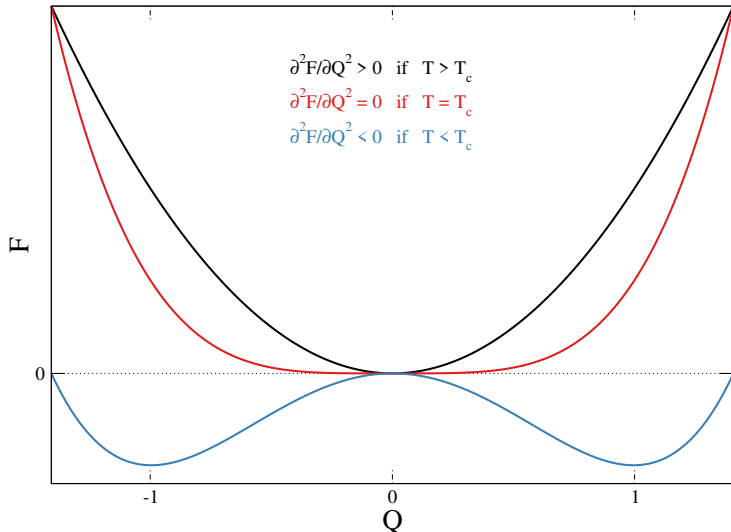
$$\mathcal{F}_H[\mathcal{H}] = \text{tr}(\rho_{\mathcal{H}} H) + \frac{1}{k_B T} \text{tr}(\rho_{\mathcal{H}} \ln \rho_{\mathcal{H}}) = F_{\mathcal{H}} + \langle V - \mathcal{V} \rangle_{\rho_{\mathcal{H}}}$$

$$F_H \leq \mathcal{F}_H[\mathcal{H}]$$

- We take a harmonic trial density matrix  $\rho_{\mathcal{H}} \equiv \rho_{\mathcal{H}}(\Phi, \mathcal{R})$ . Variables  $\Phi$  (SCHA/auxiliary phonons) and  $\mathcal{R}$  atomic centroids.
- The SCHA provides the harmonic density matrix that minimizes the free energy.

# Theoretical framework

- Landau Theory of second-order phase transitions



## Theoretical framework

- The free energy is a well defined quantity within the SCHA.
- For a given temperature, experimentally measured phonon frequencies will be centered in the phonon frequencies defined by  $\partial^2 \mathcal{F} / \partial \mathbf{R}^2$ .

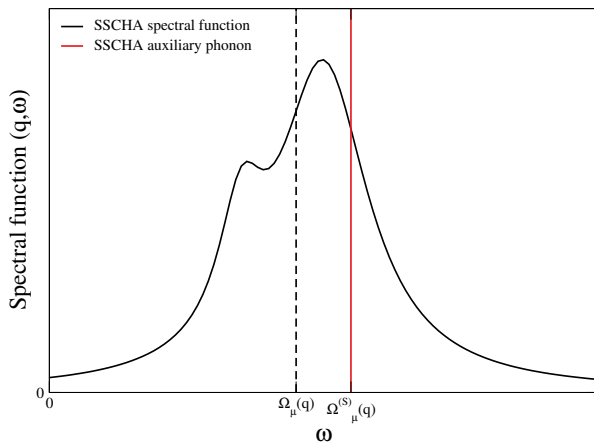
$$\frac{\partial^2 \mathcal{F}}{\partial \mathbf{R} \partial \mathbf{R}} = \Phi + \overset{(3)}{\Phi} \Lambda [1 - \overset{(4)}{\Phi} \Lambda]^{-1} \overset{(3)}{\Phi}$$

- $\overset{(3)}{\Phi} = \left\langle \frac{\partial^3 V}{\partial \mathbf{R}^3} \right\rangle_{\rho_H}$ ,  $\overset{(4)}{\Phi} = \left\langle \frac{\partial^4 V}{\partial \mathbf{R}^4} \right\rangle_{\rho_H}$ , and  $\Lambda \equiv \Lambda(\Phi)$ .
- They are different to the perturbative ones  $[\partial^3 V / \partial \mathbf{R}^3]_0$ ,  $[\partial^4 V / \partial \mathbf{R}^4]_0$

# Theoretical framework

- The static theory can be expanded by a dynamical ansatz.

$$\sigma(\mathbf{q}, \omega) = \frac{1}{\pi} \times \sum_{\mu} \frac{-\omega Im\Pi_{\mu}(\mathbf{q}, \omega)}{(\omega^2 - \Omega_{\mu}^{(S)2}(\mathbf{q}) - Re\Pi_{\mu}(\mathbf{q}, \omega))^2 + (Im\Pi_{\mu}(\mathbf{q}, \omega))^2}$$

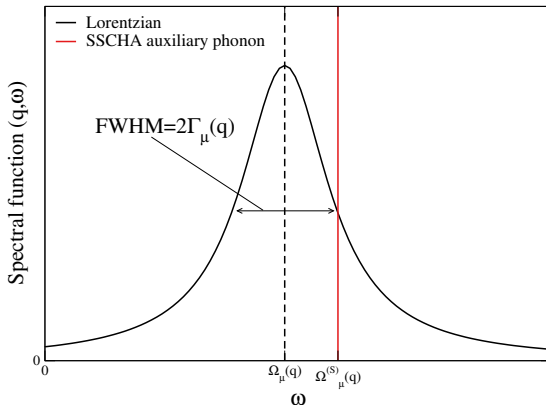


# Theoretical framework

$$\mathcal{Z}_\mu(\mathbf{q}, \omega) = \sqrt{\Omega_\mu^{(S)2}(\mathbf{q}) + \Pi_\mu(\mathbf{q}, \omega + i0^+)}$$

$$\Omega_\mu(\mathbf{q}) = \text{Re} \mathcal{Z}_\mu(\mathbf{q}, \Omega_\mu^{(S)}(\mathbf{q})),$$

$$\Gamma_\mu(\mathbf{q}) = -\text{Im} \mathcal{Z}_\mu(\mathbf{q}, \Omega_\mu^{(S)}(\mathbf{q}))$$



## Theoretical framework

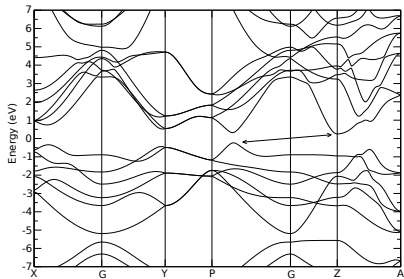
- The Lorentzian definition of phonons provides a straightforward way of calculating the lattice thermal conductivity

$$\kappa_I = \frac{1}{N_{\mathbf{q}} \Omega_{cell} k_B T^2} \sum_{\mathbf{q}\mu} v_\mu(\mathbf{q})^2 \omega_\mu(\mathbf{q})^2 n_B(\omega_\mu(\mathbf{q})) [n_B(\omega_\mu(\mathbf{q})) + 1] \tau_\mu(\mathbf{q}).$$

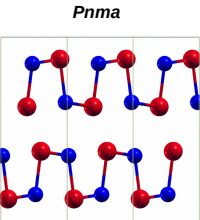
Summary:

- Anharmonic free energy
- Phase transition temperature
- Anharmonic phonons
- Lattice thermal conductivity

# SnSe

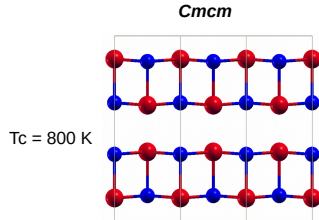


Low T, low symmetry



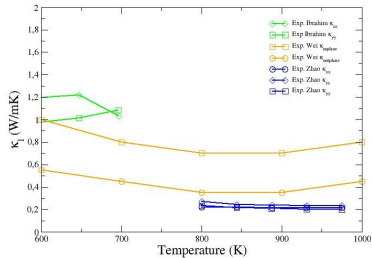
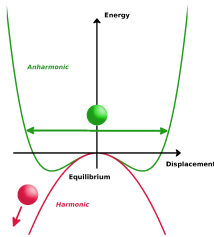
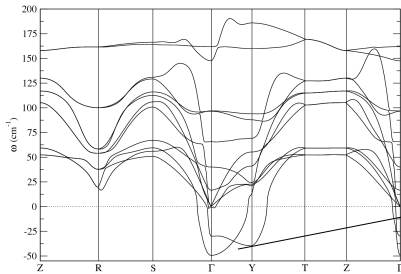
- Anisotropic crystal structure
- Narrow gap semiconductor
- Structural phase transition

High T, high symmetry



$T_c = 800 \text{ K}$

# SnSe

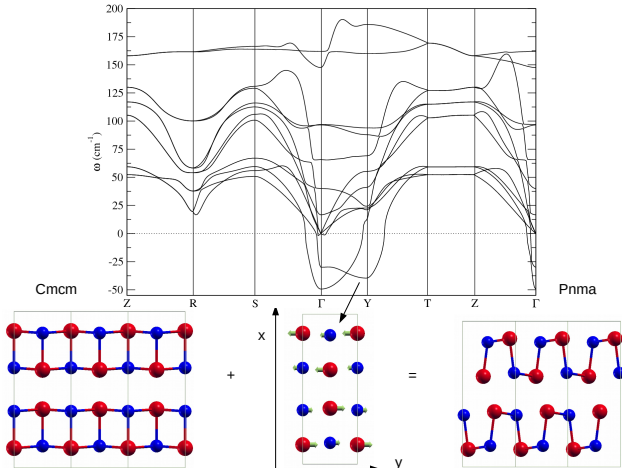


- Lattice instabilities in the harmonic approximation
- Ultralow thermal conductivity
- Experimental discrepancy
  - Value
  - Anisotropy

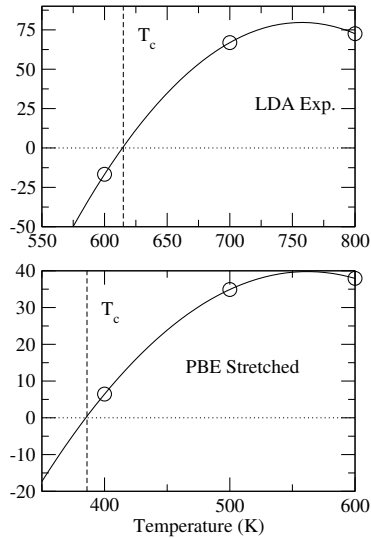
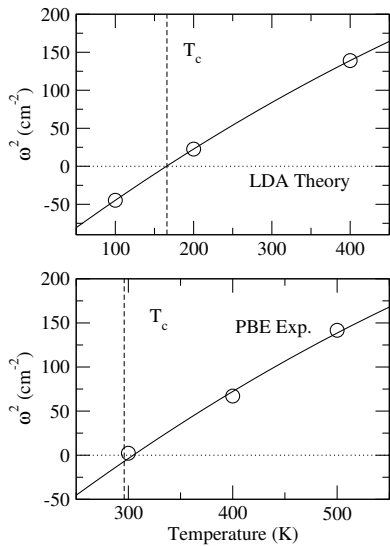
L.-D. Zhao et al. Nature 508, 373 (2014)

# SnSe

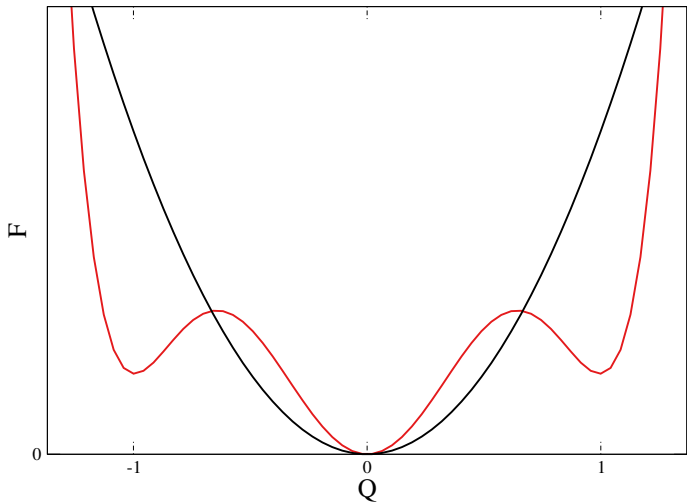
$$\frac{\partial^2 F}{\partial Q^2} \propto \omega_{Y_1}^2(T), \quad \frac{\partial^2 F}{\partial \mathcal{R} \partial \mathcal{R}} = \Phi + \overset{(3)}{\Phi} W \overset{(3)}{\Phi}, \quad \overset{(3)}{\Phi} = \left\langle \frac{\partial^3 V}{\partial \mathcal{R}^3} \right\rangle$$



# SnSe

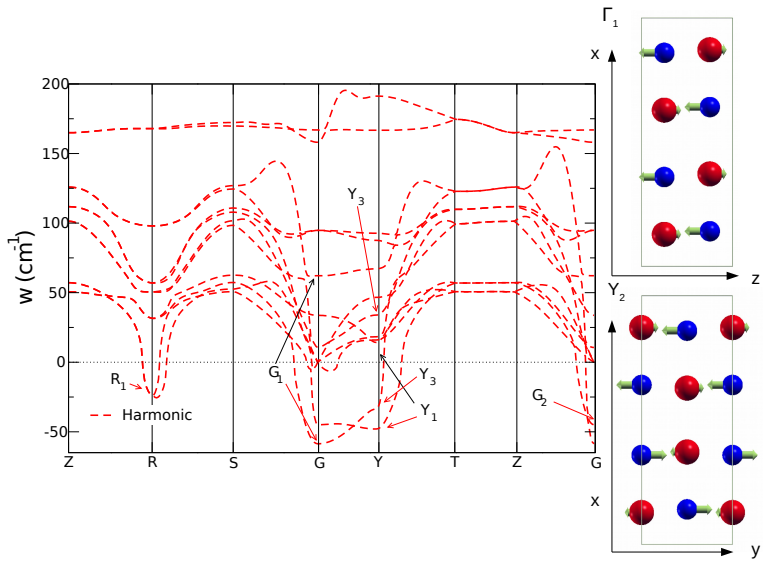


# SnSe

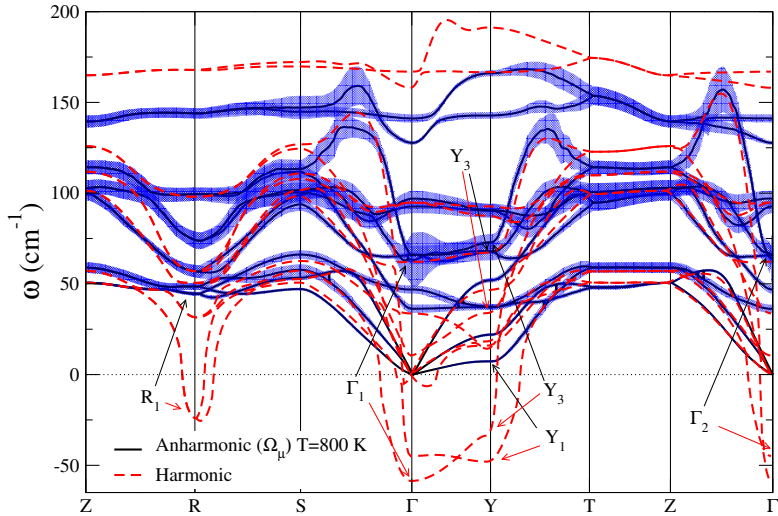


- We discard the first-order phase transition.

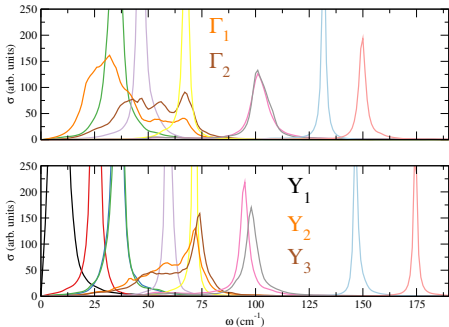
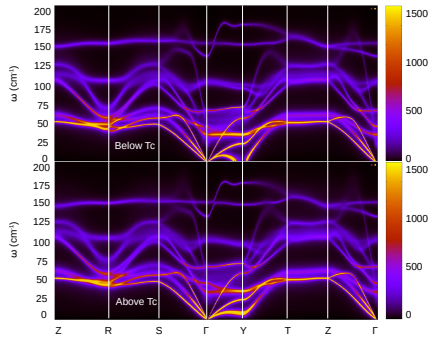
# SnSe



# SnSe



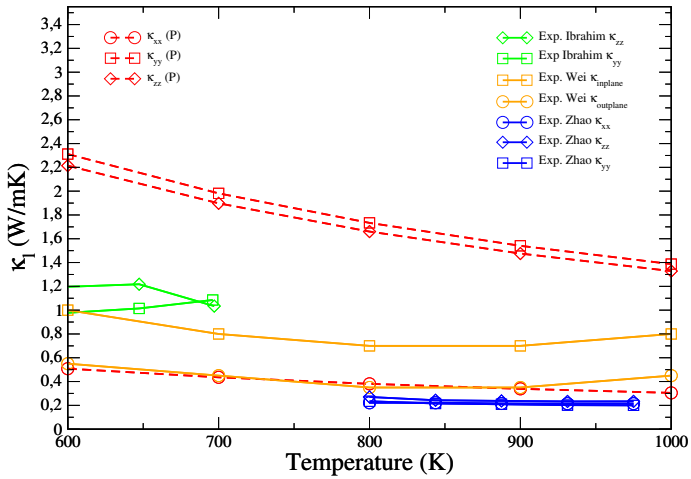
# SnSe



- The phase transition is measurable in INS experiments.
- There are modes that strongly deviate from the Lorentzian limit.

U. Aseginolaza et al. PRL 122, 075901 (2019)

# SnSe



L.D. Zhao et al. Nature 508, 373 (2014), Ibrahim et al. Appl. Phys. Lett. 110, 032103 (2017),

U. Aseginolaza et al. PRL 122, 075901 (2019)

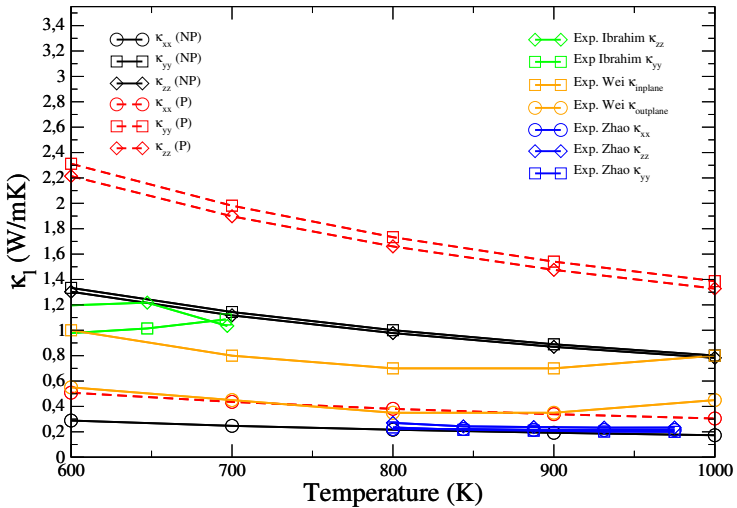
- Perturbative

$$\left[ \frac{\partial^3 V}{\partial \mathbf{R}^3} \right]_0$$

- Non-perturbative

$$\left\langle \frac{\partial^3 V}{\partial \mathbf{R}^3} \right\rangle_{\rho_{\mathcal{H}}}$$

# SnSe

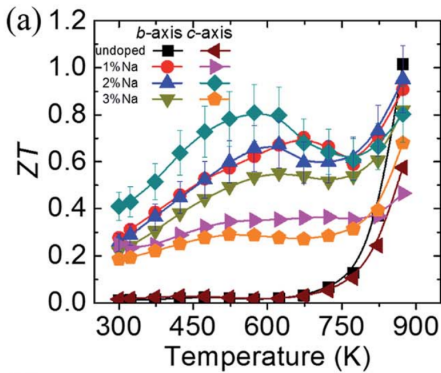
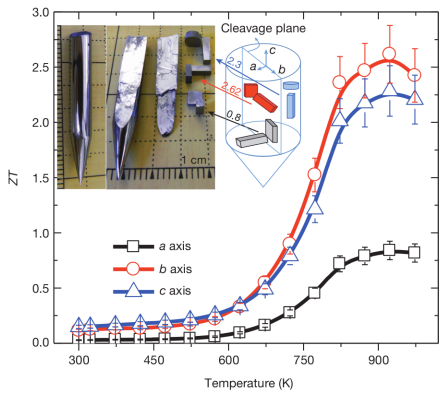


L.D. Zhao et al. Nature 508, 373 (2014), Ibrahim et al. Appl. Phys. Lett. 110, 032103 (2017),

U. Aseginolaza et al. PRL 122, 075901 (2019)

# SnSe and SnS

Left: SnSe, Right: SnS



- They look very similar thermoelectric materials.

# SnSe and SnS

$$ZT = \frac{P_F T}{\kappa}, \quad P_F = S^2 \sigma$$

$$\sigma(T, \mu) = e^2 \int_{-\infty}^{\infty} d\varepsilon \left[ -\frac{\partial f(T, \mu, \varepsilon)}{\partial \epsilon} \right] \Sigma(\varepsilon),$$

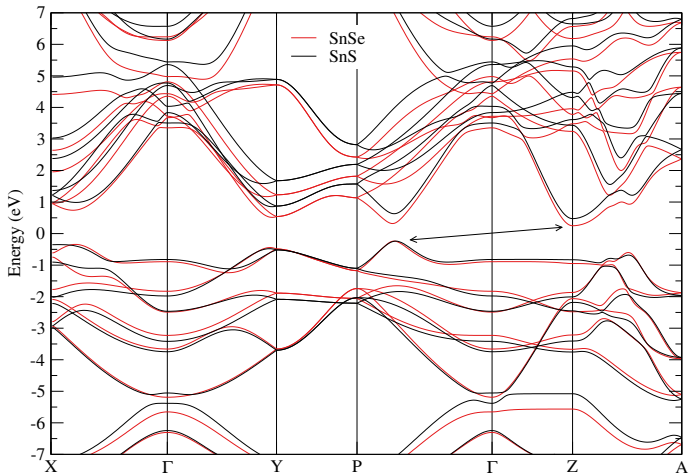
$$S(T, \mu) = \frac{e}{T \sigma(T, \mu)} \int_{-\infty}^{\infty} d\varepsilon \left[ -\frac{\partial f(T, \mu, \varepsilon)}{\partial \epsilon} \right] \Sigma(\varepsilon)(\varepsilon - \mu),$$

$$\Sigma(\varepsilon) = \frac{1}{\Omega N_{\mathbf{k}}} \sum_{n\mathbf{k}} \tau_{n\mathbf{k}}^e |\mathbf{v}_{n\mathbf{k}}|^2 \delta(\varepsilon - \varepsilon_{n\mathbf{k}}),$$

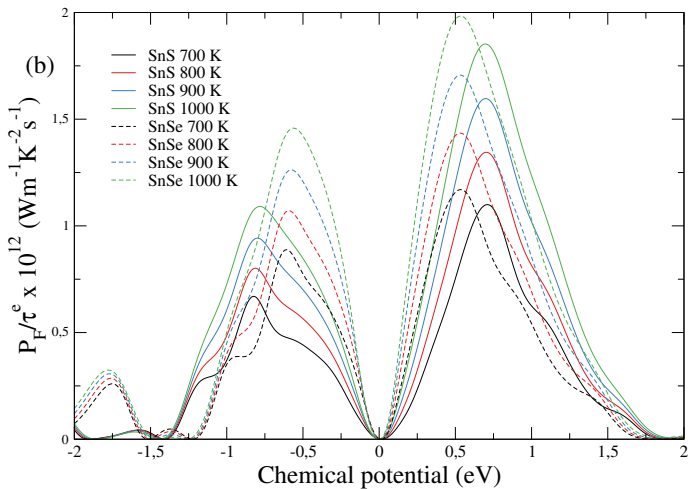
- We use the Boltztrap software package

G. K. Madsen et al. Computer Physics Communications 175, 67 (2006)

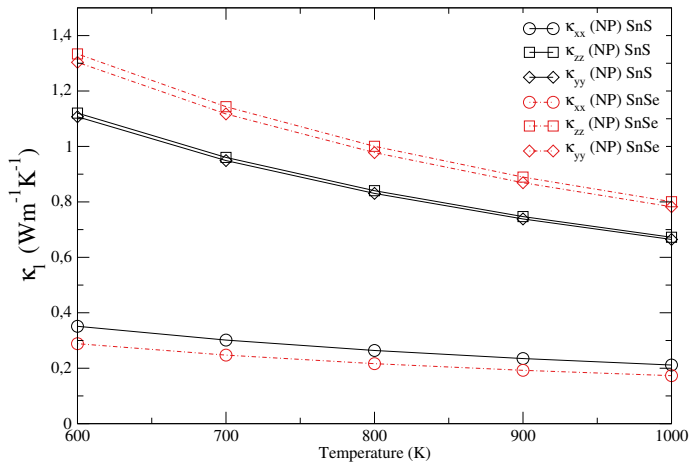
# SnSe and SnS



# SnSe and SnS



# SnSe and SnS



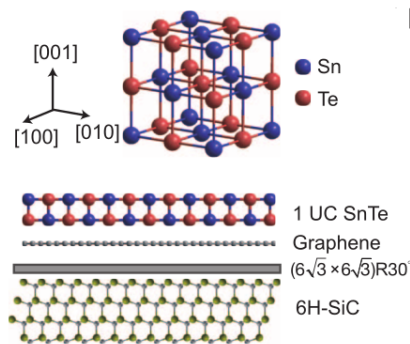
## SnSe and SnS: Conclusions

- Second-order phase transitions
- Strongly anharmonic phonon spectra
- Ultralow anisotropic lattice thermal conductivity, important non-perturbative effects
- Both materials show similar electronic and vibrational properties

# Monolayer SnSe

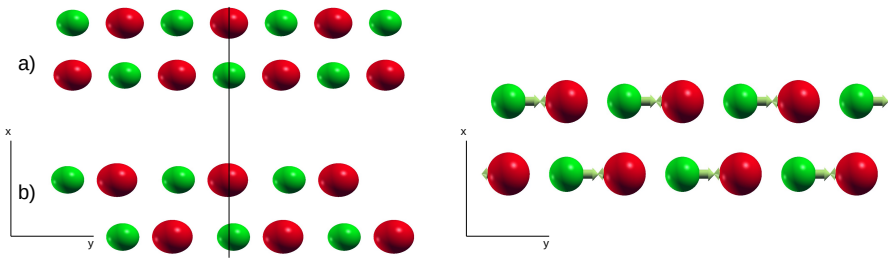
Two reasons to study monolayer SnSe:

- Theoretical calculations claim it could be an efficient thermoelectric material
- It could be an atomically thick ferroelectric material



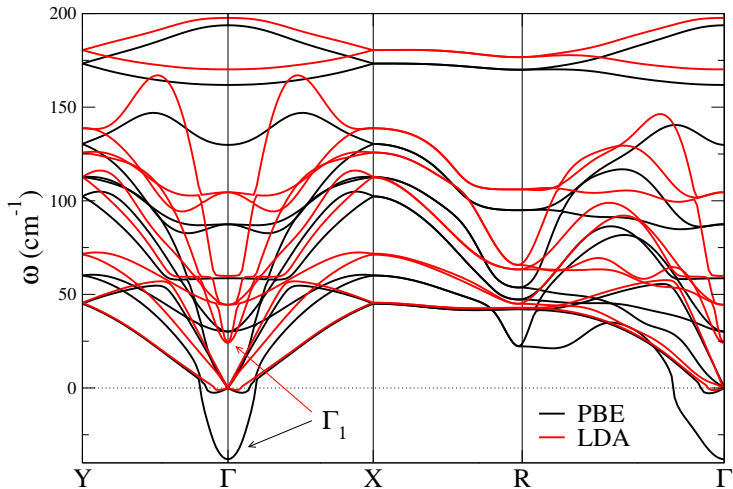
This is the case in SnTe (Kai Chang et al. Science 353, 6296 (2016))

# Monolayer SnSe



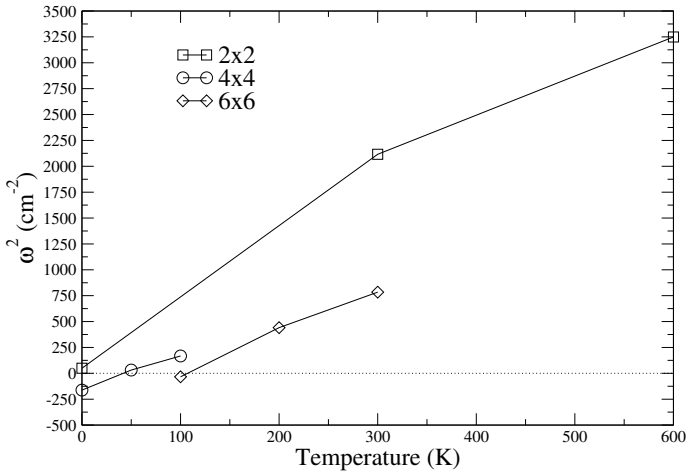
- This is the ferroelectric transition
- a) High symmetry phase ( $Q = 0$ )  $Pnmm$
- b) Low symmetry phase ( $Q \neq 0$ )  $Pnm2_1$
- Atomic displacements correspond to a phonon at the  $\Gamma$  point

# Monolayer SnSe



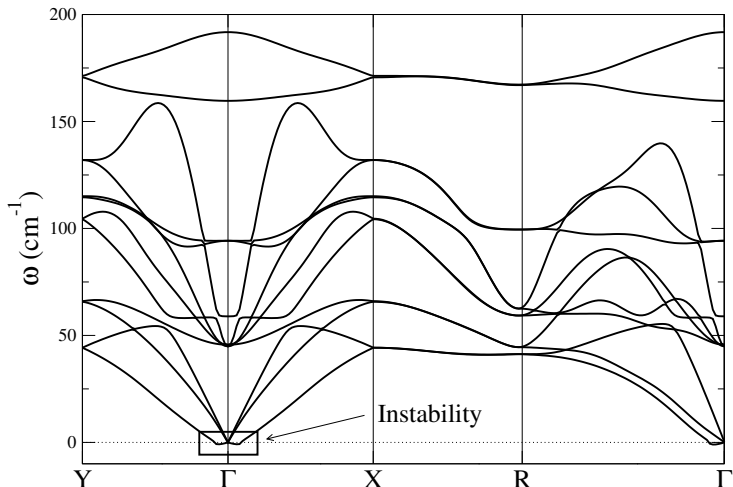
- We perform the SSCHA calculation only within PBE

# Monolayer SnSe



- Good agreement with other theoretical calculations
- Strong supercell size dependence on  $T_c$

# Monolayer SnSe



- Tiny instabilities do not allow us to compute  $\kappa_I$

# Monolayer SnSe

## Conclusions:

- We theoretically predict the ferroelectric phase transition
- Unstable Fourier interpolation of the SSCHA auxiliary phonons
  - Motivation for the study of the anharmonic effects on the lowest energy acoustic branch of 2D materials.

# Graphene

PHYSICAL REVIEW

VOLUME 176, NUMBER 1

5 DECEMBER 1968

## Crystalline Order in Two Dimensions\*

N. D. Mermin<sup>†</sup>

*Laboratory of Atomic and Solid State Physics, Cornell University, Ithaca, New York*

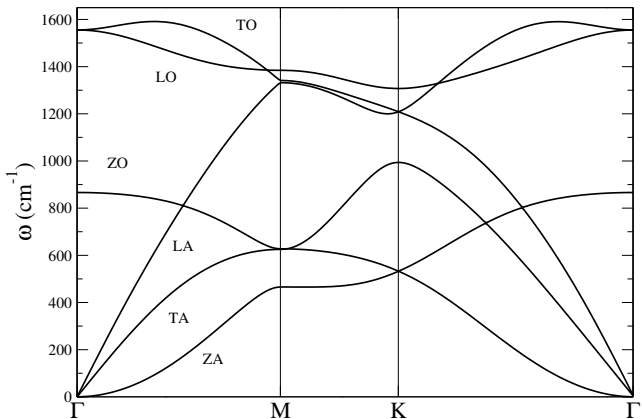
(Received 1 July 1968)

If  $N$  classical particles in two dimensions interacting through a pair potential  $\Phi(\vec{r})$  are in equilibrium in a parallelogram box, it is proved that every  $k \neq 0$  Fourier component of the density must vanish in the thermodynamic limit, provided that  $\Phi(\vec{r}) - \lambda r^2 |\nabla^2 \Phi(\vec{r})|$  is integrable at  $r = \infty$  and positive and nonintegrable at  $r = 0$ , both for  $\lambda = 0$  and for some positive  $\lambda$ .

This result excludes conventional crystalline long-range order in two dimensions for power-law potentials of the Lennard-Jones type, but is inconclusive for hard-core potentials. The corresponding analysis for the quantum case is outlined. Similar results hold in one dimension.

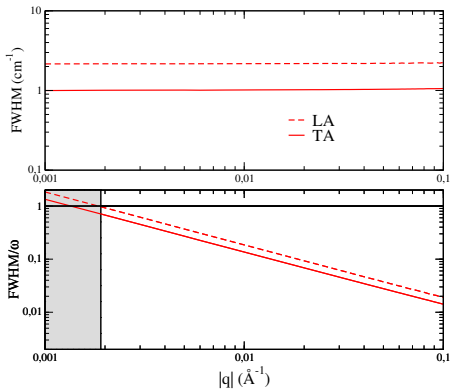
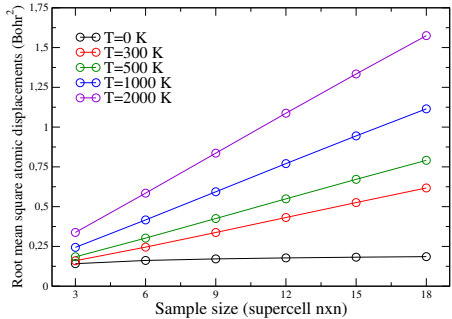
- The existence of 2D materials was not believed to be possible.
- Nowadays there is a whole branch of science exploiting their applications.

# Graphene



- $\omega_{ZA}(|\mathbf{q}|) = \alpha|\mathbf{q}| + \beta|\mathbf{q}|^2 + \dots$
- Rotational invariance (RI) together with the 2D character of  $\phi_{ab}$  makes the harmonic dispersion of mode ZA quadratic ( $\alpha = 0$ ).

# Graphene



- $\langle u^2 \rangle$  diverges for finite temperatures.
- Finite linewidths of LA/TA modes at decreasing momenta.
- Both properties arise due to the quadratic ZA modes.

# Graphene

## Hypothesis

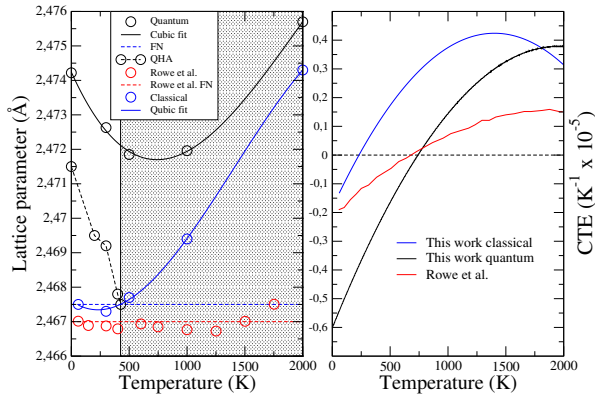
- Quadratic physical phonons are expected and compatible with the absence of divergences.

## What have we done?

- ① Perform SCHA in an atomistic model using an empirical machine learning potential trained with DFT.
- ② Perform SCHA in a continuum membrane model Hamiltonian.
  - Provides information at much smaller momenta.

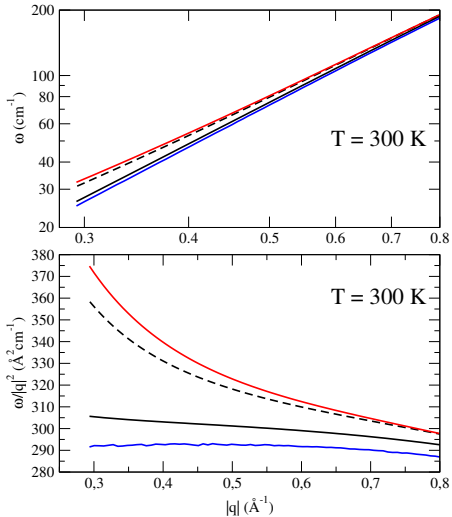
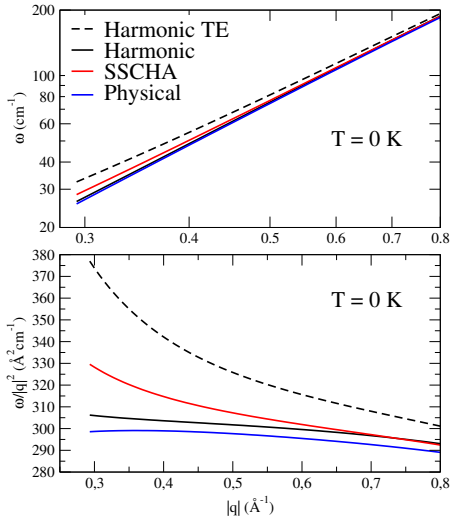
# Graphene

$$P_{\alpha\beta}^{SSCHA}(\mathcal{R}, \{\mathbf{a}_i\}) = -\frac{1}{\Omega} \frac{\partial \mathcal{F}_H[\mathcal{R}, \{\mathbf{a}_i\}]}{\partial \epsilon_{\alpha\beta}} \Big|_{\epsilon=0}$$



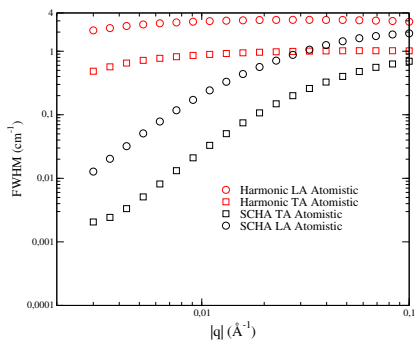
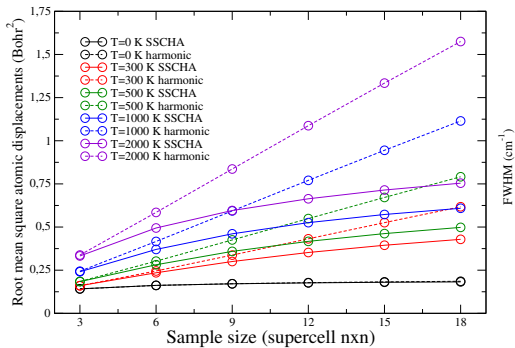
- First of all we get a strain less membrane
- Strain linearizes the ZA dispersion

# Graphene



# Graphene

- We calculate  $\langle u^2 \rangle$  using the density matrix given by the SCHA.
- We calculate the FWHM using the SCHA phonons for the three phonon scattering phase space.



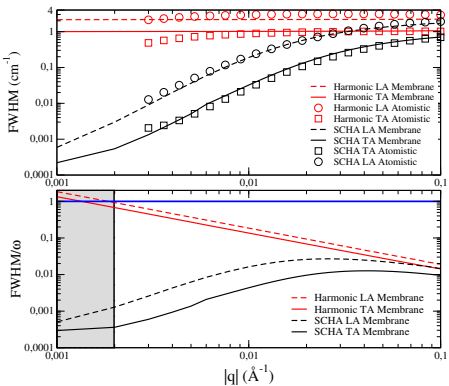
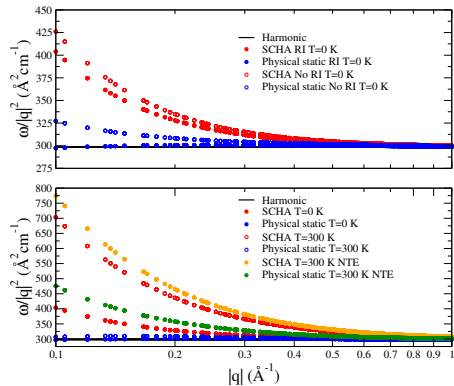
- The SCHA linearisation clearly removes the problems.

# Graphene

$$V = \frac{1}{2} \int_{\Omega} d^2x [\kappa (\partial^2 h)^2 + C^{ijkl} \partial_i u_j \partial_k u_l + C^{ijkl} \partial_i u_j \partial_k h \partial_l h \\ + \frac{C^{ijkl}}{4} \partial_i h \partial_j h \partial_k h \partial_l h + \frac{C^{ijkl}}{2} \partial_i \mathbf{u} \cdot \partial_j \mathbf{u} \partial_k h \partial_l h + C^{ijkl} \partial_i u_j \partial_k \mathbf{u} \cdot \partial_l \mathbf{u} \\ + \frac{C^{ijkl}}{4} \partial_i \mathbf{u} \cdot \partial_j \mathbf{u} \partial_k \mathbf{u} \cdot \partial_l \mathbf{u}]$$

- $u_i(x)$  where  $i = x, y$  and  $h(x)$  are the in-plane and out-of-plane displacement fields.
- $C^{ijkl} = \lambda \delta^{ij} \delta^{kl} + \mu (\delta^{ik} \delta^{jl} + \delta^{il} \delta^{jk})$  where  $\lambda, \mu$  are the Lame coefficients.
- $\kappa$  is the bending rigidity and  $\Omega$  the area of the membrane.
- $\partial_i u_j \rightarrow \partial_i u_j + \delta^{ij} \delta a$  where  $\delta a = (a - a_0)/a_0$ .

# Graphene



- SCHA phonons are linear.
- Physical phonons are quadratic.
- LA/TA linewidths decay.

# Graphene

## Conclusions:

- ① We perform simulations in strain less membranes by using the SSCHA stress tensor
- ② Anharmonicity linearises the auxiliary phonons
- ③ Divergencies removed, quasiparticle picture recovered
- ④ Physical phonons have a quadratic dispersion as expected for RI membranes.